

## ATMOSPHERIC PROPAGATION AT 100 AND 300 GHz: ASSESSMENT OF A METHOD TO IDENTIFY RAINY CONDITIONS DURING RADIOSOUNDINGS

G. A. Siles<sup>1, \*</sup>, J. M. Riera<sup>1</sup>, P. Garcia-del-Pino<sup>2</sup>, and J. Romeu<sup>3</sup>

<sup>1</sup>Dpto. de Señales, Sistemas y Radiocomunicaciones, ETSI de Telecomunicación, Universidad Politécnica de Madrid Ciudad Universitaria s/n, Madrid 28040, Spain

<sup>2</sup>Dpto. de Ingeniería Audiovisual y Comunicaciones, EUIT de Telecomunicación, Universidad Politécnica de Madrid, UPM Campus Sur, Ctra. de Valencia, km 7, Madrid 28031, Spain

<sup>3</sup>Dep. de Teoria del Senyal i Comunicacions, Universitat Politècnica de Catalunya, UPC Campus Nord, Jordi Girona 1-3, Barcelona 08034, Spain

**Abstract**—The influence of atmospheric gases and tropospheric phenomena becomes more relevant at frequencies within the THz band (100 GHz to 10 THz), severely affecting the propagation conditions. The use of radiosoundings in propagation studies is a well established measurement technique in order to collect information about the vertical structure of the atmosphere, from which gaseous and cloud attenuation can be estimated with the use of propagation models. However, some of these prediction models are not suitable to be used under rainy conditions. In the present study, a method to identify the presence of rainy conditions during radiosoundings is introduced, with the aim of filtering out these events from yearly statistics of predicted atmospheric attenuation. The detection procedure is based on the analysis of a set of parameters, some of them extracted from synoptical observations of weather (SYNOP reports) and other derived from radiosonde observations (RAOBs). The performance of the method has been evaluated under different climatic conditions, corresponding to three locations in Spain, where collocated rain gauge data were available. Rain events detected by the method have been compared with those precipitations identified by the rain gauge. The pertinence

---

*Received 26 June 2012, Accepted 31 July 2012, Scheduled 15 August 2012*

\* Corresponding author: Gustavo Adolfo Siles Soria (gsiles@grc.ssr.upm.es).

of the method is discussed on the basis of an analysis of cumulative distributions of total attenuation at 100 and 300 GHz. This study demonstrates that the proposed method can be useful to identify events probably associated to rainy conditions. Hence, it can be considered as a suitable algorithm in order to filter out this kind of events from annual attenuation statistics.

## 1. INTRODUCTION

The THz band covers a broad spectral range comprised between 100 GHz and 10 THz, which corresponds to wavelengths going from 3 mm to 30  $\mu\text{m}$ , respectively. Within this range, a considerable research effort is currently concentrated on technological developments aiming to improve characteristics and performance of devices for emitter and receiver systems. A very important number of comprehensive reviews [1, 2] on the state-of-the-art of THz technology [3–5] can be found in the literature. A non-exhaustive list of applications includes astronomy [6], security scanning [7], explosives detection [8], medical imaging and biology [9, 10] and atmospheric remote sensing [11].

High frequencies have also attracted the attention of the Earth-to-space propagation community and some interesting works studying the effect caused by atmospheric gases, clouds, rain and scintillation have already been reported [12–14]. Although there is a lack of experimental data from measurements campaigns above the Q band, and no satellites at these frequencies are envisaged in the near future, propagation scientists are starting to work in this field, in order to contribute to address new system requirements or redefine frontiers for future applications.

The TeraSense project [15] is a collaborative initiative, coordinated by Universitat Politècnica de Catalunya (UPC), joining the efforts of sixteen Spanish research teams specialized into different scientific and technological areas. Within this framework, a series of studies are being developed at Universidad Politècnica de Madrid (UPM), including measurements of antennas, design of circuits, and simulation and modelling of radiation-matter interaction. In particular, within the propagation domain, the effects of atmosphere under non-scattering conditions at 100 GHz and 300 GHz are being studied at UPM in order to gain a better understanding about qualitative and quantitative aspects.

From a point of view of the propagation medium, the present work is concentrated on a non scattering atmosphere, where atmospheric gases and clouds are the most important contributors of radiation absorption effects. Gaseous attenuation is evaluated as the sum of the

effects of water vapor and oxygen, using well established physically-based models, as the proposed by Liebe et al. [16] or Rosenkranz [17]. Cloud attenuation can be evaluated under the Rayleigh approximation, which is considered valid up to 300 GHz for small water particles, typically those with radii below 30  $\mu\text{m}$  [18], non associated to rainy conditions. Therefore, absorption caused by water droplets in clouds can be considered independent of their droplet size distribution and can be linearly related to cloud liquid water density. The estimation of this parameter, as well as the detection of cloud layers, can be performed through a variety of cloud detection algorithms detailed in the literature [19–21].

The use of meteorological radiosoundings is one of the most accepted techniques allowing atmospheric temperature, pressure and relative humidity profiles, among others, to be collected. Radiosonde launches are typically carried out in specific sites, twice or four times every day. During its ascent from the surface up to a height of about 30 km, the balloon transmits measurements to a receiver installed on a ground launching station. Radiosonde observations (RAOBs) data are easily accessible [22] and enormous compilations of quality-assured datasets from around the World are also available for the propagation community [23]. Vertical meteorological profiles extracted from RAOBs are the input variables for the above mentioned attenuation estimation models. However, strong scattering effects caused by the interaction between high frequency radiation and water droplets are not evaluated by cloud attenuation models, which are fundamentally based on the effects of radiation absorption, and not on scattering processes. Thus, with the aim of computing degradations through a non-precipitating medium at 100 and 300 GHz, the probable presence of rainy conditions during radiosoundings is a relevant aspect to be analyzed. Considering that RAOBs data do not provide a direct numerical parameter allowing events to be classified as rainy or non-rainy, the main goal of the present paper is to propose and assess a method using information extracted from RAOBs and colocated synoptical observations of weather (SYNOP reports), in order to identify and filter out those radiosoundings. The issue of detecting rainy periods is relevant in propagation campaigns and has already been discussed by other authors, using with this purpose measurements of sky brightness temperature collected by dual-frequency radiometers [12, 24].

In our work, an important volume of meteorological information, including RAOBs data, SYNOP reports and rain gauge data, has been used to define and evaluate the rain detection method. Some relevant aspects concerning the different meteorological data sources are briefly

summarized in Section 2. Then, a detailed description of the proposed rain detection method is discussed in Section 3. Assuming that a rain gauge colocated at the same site of radiosonde launches could provide more accurate information about the presence or absence of rain, in Section 4 the method is validated using rain data extracted from rain gauge records. Following this evaluation process, the method is used in order to compute of 5-years statistics of total attenuation at the frequencies of interest in Section 5; it is expected that cumulative distributions obtained in this way would be closest to the ones obtained by experimental techniques under non-precipitating conditions. At the end of the present paper, some conclusions are summarized and discussed.

## 2. METEOROLOGICAL DATA

A variety of meteorological data is regularly registered in specific weather stations in Spain. In particular, RAOBs data, SYNOP reports and precipitation information from rain gauges, are of interest for the present study. In order to assess the performance of the rain detection method under different climatic conditions, three different sites have been selected for this study. More specifically, available datasets have been collected from the following weather stations: Madrid/Barajas (08221), Murcia (08430) and Santander (08023). The site codes correspond to the station numbering system of the World Meteorological Organization (WMO). Relevant information about the stations is given in Tables 1 and 2.

### 2.1. Radiosoundings

Radiosonde balloons are launched routinely twice a day (00:00 and 12:00 UTC) at the stations shown in Table 1, as in most of the launching stations coordinated with WMO. Some sporadic soundings at different times (06:00 and 18:00 UTC) have been detected and discarded from the following stages of analysis, for the sake of data regularity. The preprocessing of raw vertical profiles includes validation and checking procedures in order to identify non-existing or invalid soundings. With this purpose, a series of software routines have been implemented, which are responsible of the following verification tasks:

- Checking of minimum and maximum height levels attained by the radiosonde.
- Detection of repeated height values.
- Detection of inversions of height or pressure levels.

**Table 1.** Station locations and climate characteristics.

Site	Location	Coordinates			Climate
		Lat (N)	Long (W)	Alt (m)	
1	Madrid/Barajas	40.45	03.57	631	Continental
2	Murcia	38.00	01.17	61	Mediterranean
3	Santander	43.48	03.80	52	Maritime

**Table 2.** Meteorological data and periods of availability.

Site	Annual Rainfall (mm)	Days with Precipitation	Meteorological Data (Time Period)		
			RAOBs	SYNOP	Rain Gauge
1	436	63	2007–2011	2007–2011	2010–2011
2	339	33	2002–2003	2002–2003	2002–2003
3	1246	128	2010–2011	2010–2011	2010–2011

- Checking of missing values of temperature, pressure or height levels.

Finally, assuming a layered atmosphere model, temperature, pressure and relative humidity values are calculated for a set of defined height levels, through an interpolation procedure, using as input the preprocessed radiosounding data.

## 2.2. SYNOP Observations

Surface synoptic observations are reported at the manned stations of Table 1 four times a day (00:00, 06:00, 12:00 and 18:00 UTC). As they are well-standardized by the WMO, the information about meteorological conditions provided by these reports is coded according to the alpha-numeric data format FM-12 [25].

A decoding process of these raw data is carried out with the aim of extracting useful meteorological information. In particular, relevant information relative to the presence of rain events is extracted from the following decoded parameters [25]:

- SYNOP Present Weather parameter (*ww* code): Numerical code describing weather conditions at observation time.
- SYNOP Liquid Precipitation parameter (*RRR* code): It represents the liquid precipitation amount in (mm) during the previous 6 h, for SYNOP reports registered at 00:00 and 12:00 UTC, or the previous 12 h, for those ones collected at 06:00 and 18:00 UTC before the SYNOP observation. As a consequence,

information on accumulated rain within 6-hour intervals can be derived from the analysis of this parameter.

### 2.3. Rain Gauge

Time series of accumulated rain, expressed in (mm), with an integration time of 10 minutes, have been provided by the public Spanish meteorological agency, AEMET, for the periods of time detailed in Table 2. This source of information has been used in order to evaluate the rain detection method by comparing its results with those rainy periods identified by the rain gauge.

## 3. RAIN DETECTION METHOD

In this section, a new rain detection method is proposed in order to identify and filter out those radiosoundings probably carried out during rainy conditions. The method has been developed on the basis of an analysis of meteorological data from Madrid/Barajas station.

### 3.1. Analysis

A first analysis allows to extract the following considerations that have been taken into account for defining the method:

- The frequency-independent parameter ILWC (Integrated Liquid Water Content), expressed in (mm), measures the amount of liquid water along the radiosounding path. The ILWC value is calculated integrating the liquid water content,  $w_c$  in ( $\text{gm}^{-3}$ ) along the considered path. Since RAOBs do not provide a direct measurement of the parameter  $w_c$ , it has to be estimated using one of the cloud detection models referenced in Section 1.
- As a first approach, given a series of yearly atmospheric profiles from RAOBs, the value of ILWC could be considered as the more suitable indicator in order to get information about the presence of rainy conditions. However, as far as we know, it is not possible to easily separate rain and non-rain events only by analyzing the value of ILWC for each profile.
- In order to detect the presence of rain on the site under study, colocated rain gauge data could be considered the most reliable source of information. However, rainfall data measured by this kind of instruments is not always available.
- In the absence of colocated rain gauge data, SYNOP reports, widely available, can be evaluated in order to identify rainy conditions during radiosoundings.

### 3.2. Description of the Method

The following set of detection criteria is used in the method:

- (i) Criterion 1 ( $CR_1$ ) is defined on the basis of the SYNOP Present Weather parameter. According to the standardized decoding schemes of this indicator [25], SYNOP records whose numerical codes ( $ww$ ) correspond to drizzle (50–59), rain (60–69), showers (80–89) or thunderstorm (90–99) events have been marked as precipitation events. Codes associated with snow (70–79) events could also be considered in other climatic regions.
- (ii) Criterion 2 ( $CR_2$ ) is based on the presence of rain in 6 h previous to the radiosonde launching. This information is obtained from the SYNOP Liquid Precipitation parameter ( $RRR$ ), as it was explained in Section 2. A probable rainy condition is identified if the accumulated amount of liquid precipitation is higher than 1 mm.
- (iii) Criterion 3 ( $CR_3$ ) is based on the presence of rain in 6 h after the radiosonde launching, also obtained from the SYNOP Liquid Precipitation parameter ( $RRR$ ). As in the  $CR_2$ , a probable rain event is detected if the accumulated precipitation exceeds 1 mm.
- (iv) An ILWC threshold is introduced with the aim of evaluating those probably false rain events, characterized by very low ILWC values and detected by  $CR_2$  and  $CR_3$ , which may correspond to precipitation occurred not simultaneously with the radiosonde flight. Then, the threshold  $ILWC_{th} = 0.1$  mm has been defined. Below this value, the presence of thin cloudy conditions [26] can be assumed, which would not be responsible of precipitations.
- (v) Thus, the ILWC values lower than  $ILWC_{th}$  are not considered as precipitations, with exception of those detected by  $CR_1$ . To the best of our knowledge, this criterion should be established

**Table 3.** Summary of rain detection criteria based on SYNOP parameters.

Criterion	Description
$CR_1$	Present Weather Parameter ( $ww$ ): Rain at Observation Time
$CR_2$	Liquid Precipitation Parameter ( $RRR$ ): Accumulated Rain in previous 6 h > 1 mm
$CR_3$	Liquid Precipitation Parameter ( $RRR$ ): Accumulated Rain in following 6 h > 1 mm

as the most reliable identifier of presence of rain during a radiosounding.

The identification criteria are summarized in Table 3. Finally, a rain event is detected if at least one of the following conditions is verified:

- (i)  $CR_1$  is satisfied during SYNOP observation.
- (ii)  $ILWC > ILWC_{th}$  during events verifying  $CR_2$  or  $CR_3$ .

### 3.3. Application of the Method

To illustrate the use of the method, RAOBs and SYNOP records from year 2007 have been used as input data. Concurrent radiosonde launches and synoptical observations have been selected. For this period, a total of 628 events out of a total of 662 have been analyzed.

The ILWC corresponding to each vertical profile has been computed by numerical integration of  $w_c$ . Due to the good behavior of the Salonen model [19] in Madrid's climate, observed during previous propagation experiments [27], it has been used to detect the presence of clouds and estimate the value  $w_c$ . The yearly time series of ILWC for the period under study is shown in Fig. 1(a). Clear sky or thin cloudy conditions are characterized by zero or very low values of ILWC; however, the presence or absence of rain is not easily identified by visual inspection.

Events detected by using  $CR_1$  have been plotted on the ILWC time series, as it can be seen in Fig. 1(b). A first visual analysis allows to distinguish that several events correspond with high ILWC values. However, it can be also observed that some ILWC peak values (blue circles in the same plot) are not identified by this criterion. They could probably be related to rain events that affected the sounding measurement, but that occurred earlier or later than the SYNOP present time observation. As the radiosonde ascent may take up to one hour in some cases, both meteorological measurements are not strictly simultaneous. The criteria  $CR_2$  and  $CR_3$  have been designed in order to deal with these cases.

Rainy events identified by using  $CR_2$  and  $CR_3$  are plotted on the ILWC time series in Figs. 1(c) and 2(a), respectively. Some of the events detected with these criteria present very low values of ILWC (blue circles in both figures), which are not commonly associated with rainy events. As it was explained in the previous subsection, a refinement based on the use of an ILWC threshold has been included in order to evaluate these particular cases.

All the events detected by the three criteria have been plotted in Fig. 2(b), as well as the threshold  $ILWC_{th}$ . Events are classified

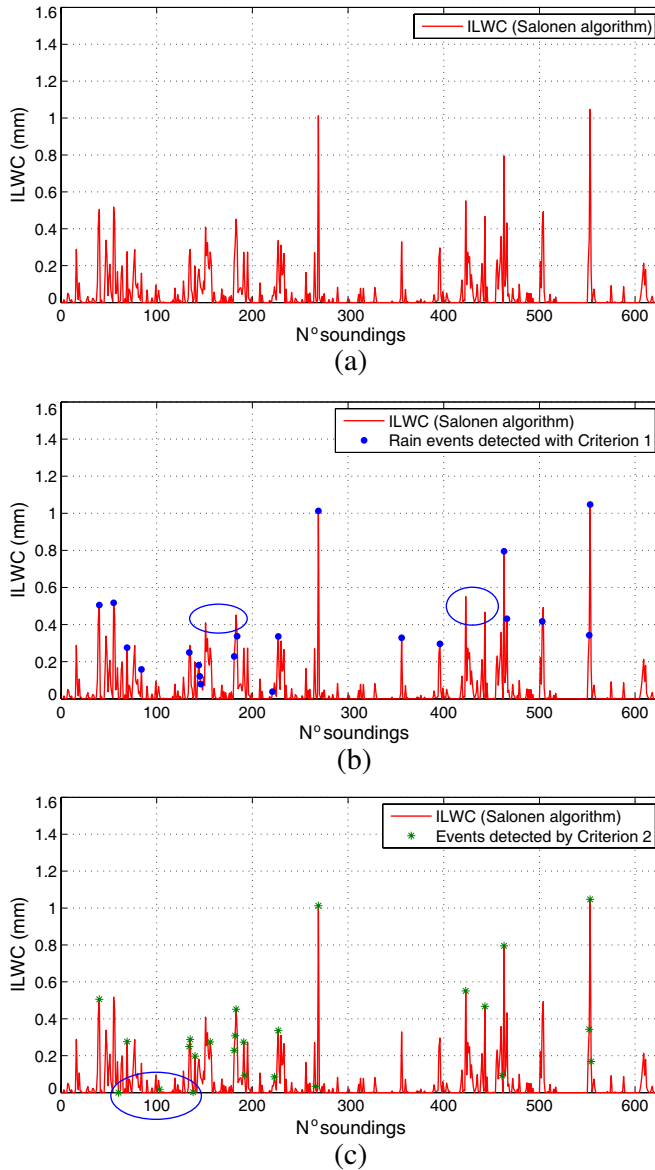


**Figure 1.** Evaluation of the method of identification of rain events using SYNOP parameters. (a) Yearly time series of ILWC. (b) Rain events detected by  $CR_1$ , some high ILWC values are not detected by this criterion. (c) Rain events detected by  $CR_2$ . Madrid/Barajas. Year 2007.

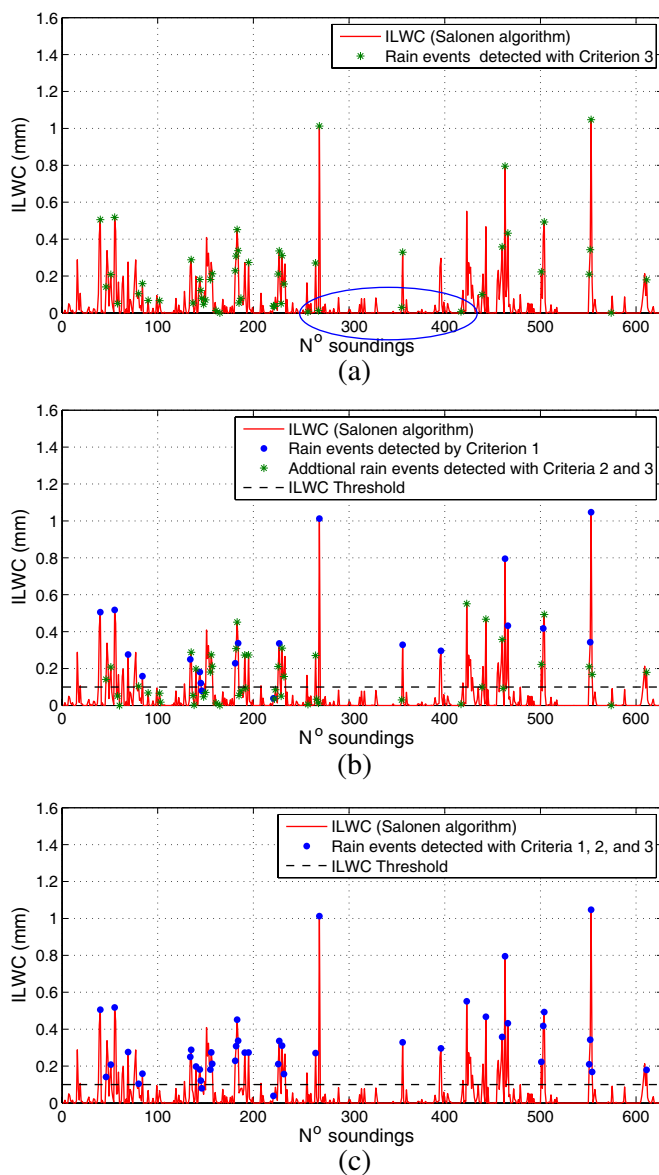


**Figure 2.** Evaluation of the method of identification of rain events using SYNOP parameters. (a) Rain events detected by  $CR_3$ . (b) Events detected by all criteria and definition of the threshold  $ILWC_{th}$ . (c) Final rain events detected by the method. Madrid/Barajas. Year 2007.

according to the following order of detection: a) precipitations observed by  $CR_1$ , b) additional events identified by the combination of  $CR_2$  and  $CR_3$ .

Finally, all rain events identified by the method have been plotted in Fig. 2(c). The difference with Fig. 2(b) is that events detected by  $CR_2$  and  $CR_3$  are only kept if they verify  $ILWC > ILWC_{th}$ .

Similar analysis based on time series of ILWC have also been carried out in Madrid/Barajas, for years 2008 to 2011. In general terms, comparable behaviors have been observed, leading to validate the detection criteria and the whole method above proposed. Additionally, the use of non colocated rain-gauge data aiming to improve the procedure has also been tested, however significant refinements on the identification of rain events have not been verified [28].

## 4. EVALUATION OF THE METHOD

### 4.1. Identifying Events Using Colocated Rain Gauge Data

With the aim of evaluating the accuracy of the proposed rain detection method, a comparative study has been carried out using available colocated rain gauge data. Yearly time series of accumulated rain, expressed in (mm), with an integration time of 10 minutes have been analyzed in order to identify the presence of rain during the launching and ascent of the radiosonde balloon. With this purpose, the following considerations have been taken into account:

- Launching of radiosondes is not always carried out on time. According to [29], balloons are usually launched between 45 and 30 minutes earlier than the nominal time reported in meteorological literature, typically at 00:00 and 12:00 UTC.
- In addition to this important issue, the time elapsed until the radiosonde reaches a theoretical rain height, typically assumed in Madrid as 3.0 km amsl [30], must be taken into account. As a first approximation, with the aim of estimating this time interval, a balloon ascent constant velocity of 300 m/min has been considered [29].
- Thus, a time interval of 70 minutes before and 20 minutes after the theoretical launching time is proposed. A rain event is considered existent as long as the rain amount in the rain gauge is higher than or equal to 0.1 mm within this 90-minutes period.

## 4.2. Comparative Analysis between the Method and the Identification by Rain Gauge Data

A comparison of the number of events detected by the proposed method and those identified from rain gauge data has been carried out and is extensively discussed in the following paragraphs.

### 4.2.1. Yearly Time Series Analysis

A first evaluation has been carried out using data of year 2011 in Madrid/Barajas. As it is shown in the yearly time series of ILWC given in Fig. 3(a), 38 out of 659 meteorological profiles have been identified as corresponding to rainy conditions, by using the proposed method. These events are clearly identified in the plot.

Then, the presence of rainy conditions has been evaluated using collocated rain gauge information for the same period of time. A total of 23 radiosoundings have been identified as carried out under rainy conditions and they have been plotted on the ILWC time series previously obtained, as it is shown in Fig. 3(b). Some missing rain gauge data, coincident with RAOBs, have also been observed during the analysis and are also plotted on the time series.

A first visual comparison between Figs. 3(a) and 3(b) allow to observe a good agreement on the detection of events, specially for those characterized by ILWC values above 0.1 mm. Below this threshold, the rain gauge hardly ever identifies rainy conditions. This fact would allow to preliminary conclude that the choice of this value for  $ILWC_{th}$  can be assumed as adequate.

### 4.2.2. Comparative Analysis for 3 Different Sites

As it was summarized in Table 2, collocated rain gauge data is available for different periods and geographical sites having different climate conditions. It provides a valuable opportunity for evaluating the performance of the method and validating the proposed procedure through a comparative analysis similar to the one discussed above for Madrid/Barajas. As a general rule being applied in this assessment, the rain events detected by the method not having time-coincident rain gauge information have been eliminated from the comparison study.

Due to the volume of data considered in this analysis, the results obtained are reported in tabular form in Table 4. A first observation is related to the number of events detected, regardless the method that has been used. Santander presents the highest number of events detected, as it is also the site with the highest number of rainy days along the year and the highest amount of precipitation (see Table 2).

Madrid and Murcia are much drier than Santander, which is clearly reflected in Table 4, as well as the fact that Murcia has the lowest number of rainy days.

After examining the results obtained, an important observation is related to the number of radiosoundings to be filtered out using the proposed method, which is always higher than those ones identified by the precipitation data given by the rain gauge. Thus, the method is conservative in that it identifies, and would lead to discard, some events that are not associated to precipitations registered by the rain gauge. This kind of events is detected by CR<sub>2</sub> and CR<sub>3</sub> and corresponds to rainy clouds that would lead to precipitation during the previous or following six hours.

On the other hand, there is a number of rain events detected

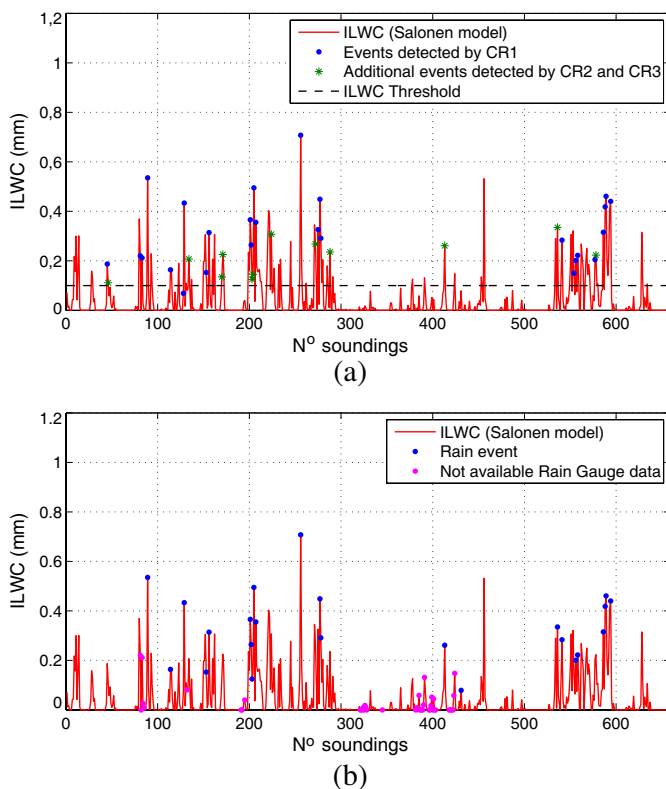


**Figure 3.** Rain events identified by (a) CR<sub>1</sub>, CR<sub>2</sub> and CR<sub>3</sub>, using  $ILWC_{th} = 0.1$  mm, and (b) collocated rain gauge data. Madrid/Barajas. Year 2011.

**Table 4.** Summary of rain detection comparative study using SYNOP criteria and rain gauge data for 3 different sites and time periods.

Location	Period	Total RAOBs with SYNOP	Events detected		Coincident events
			proposed method	colocated rain gauge	
Madrid/Barajas	2010	695	55	41	33
Madrid/Barajas	2011	659	36	23	22
Murcia	2002	665	26	23	19
Murcia	2003	687	34	26	21
Santander	2010	620	89	78	57
Santander	2011	669	63	46	37

by the rain gauge that are not detected by the method. Assuming that the analysis of rain gauge data could be considered as the most reliable source of information about the presence of rain, it is observed after a cross verification procedure, that between 75% and 95% of the events detected by this instrument have been identified by the method. Lower percentages of accuracy of detection are associated to Santander station whereas better results correspond to Madrid and Murcia locations. The relevance of the events missed by the method is discussed in the following subsection.

### 4.3. Evaluation Based on CCDFs of Total Atmospheric Attenuation at 100 GHz and 300 GHz

The Complementary Cumulative Distribution Functions (CCDF) of total attenuation,  $A_T$  (dB), along a zenith path have been calculated at 100 GHz using all valid vertical profiles collected from RAOBs in Madrid/Barajas and Santander stations, for the period of 2011, and at Murcia station for the year 2002. Results are shown in Figs. 4(a), 4(b) and 4(c), respectively. Under non-precipitation conditions, the value of  $A_T$  can be expressed as the sum of attenuation caused by atmospheric gases  $A_G$  (dB) and clouds  $A_C$  (dB) [33].

Assuming a stratified and homogeneous atmosphere model,  $A_G$  can be expressed by the sum of the attenuation at each individual atmospheric layer. Each one has a thickness and a specific attenuation  $\alpha_G$  in (dB/km). The values of  $\alpha_G$  have been computed using the line-by-line calculation included in ITU-R Rec. P.676 [31]. Therefore, the corresponding value of  $A_G$  for each sounding is computed by numerical integration. A similar approach has been used to estimate the value of  $A_C$ . The integration of the different values of cloud specific attenuation

$\alpha_C$ , expressed in (dB/km), is carried out along the sections of the zenith path where clouds have been detected by the Salonen cloud detection algorithm [19]. The corresponding values of  $\alpha_C$  have been calculated under the assumption of the validity of the Rayleigh regime at the frequencies of interest, using the analytic expressions proposed in ITU-R Rec. P.840 [32]. As it was detailed in a previous work [18], absorption due to the presence of non-rainy clouds can be evaluated under the Rayleigh approximation, which is considered valid up to 300 GHz for clouds containing spherical and small water particles, typically with radii below 30  $\mu\text{m}$ .

The identification method of rain events has been used in order to filter out those RAOBs carried out during rainy conditions. Then, a new set of CCDFs of total attenuation have been computed with those

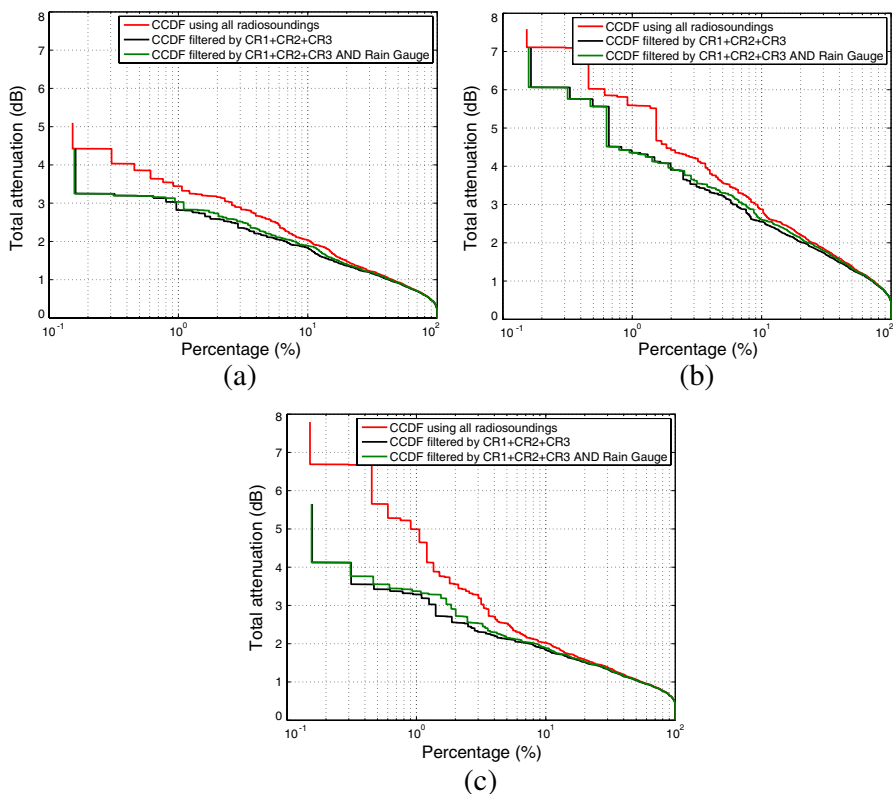


**Figure 4.** Set of three CCDFs of total attenuation at 100 GHz for (a) Madrid/Barajas, year 2011, (b) Santander, year 2011, and (c) Murcia, year 2002.

non-discarded events and plotted in Figs. 4(a), 4(b) and 4(c) (black curves). These statistics are compared with those obtained from all radiosoundings (red curves).

At this point of the study, some observations are relevant. The behavior of yearly statistics of total attenuation exceeded for high percentages of time, typically associated to effects of gaseous absorption, are not notably affected by the filtering process. Nevertheless, the effect of discarding radiosoundings is clearly noticed below 10% of the time, where the effect of liquid water content into clouds becomes more relevant. Below 1% of the time, where rain attenuation is the main propagation impairment, the values observed could be related to the sporadic presence of clouds with high ILWC values.

As it was pointed out during the comparative analysis shown in Table 4, a higher number of events are classified as rain events by the proposed rain detection method with respect to those identified by the rain gauge. With the aim of gaining a better understanding of the effect of this difference on the results, additional CCDFs of total attenuation have been computed discarding only the events jointly detected by the rain gauge and the method. The resulting CCDFs for the three different sites have also been plotted in Figs. 4(a), 4(b) and 4(c) (green curves).

After examining the set of the three first-order statistics for each site, it can be observed that although some additional events have been discarded by the method, the two filtered CCDFs (green and black curves) are quite similar. Only small differences are observed for total attenuation values exceeded between 2% and 20% of time. This comparison supports the conclusion that, in the absence of rain gauge data, the method based on SYNOP criteria can be a valuable tool of identification in order to evaluate the presence of rain during RAOBs. Using this method, yearly statistics are not significantly different to the ones obtained with a procedure based on colocated rain gauge data.

Furthermore, no significant differences are observed below 2% of the time. It can be concluded that these tails of the distributions are related to the presence of clouds with high liquid water content. The presence of rain is discarded both by the proposed method as well as by the analysis of colocated rain gauge data.

A similar analysis has been carried out at 300 GHz in order to evaluate the effect of the method on yearly statistics of total attenuation at this frequency. In the same way as in the case at 100 GHz, the set of 3 CCDFs has been computed, extracting the same events identified as rainy conditions. Results are shown in Fig. 5 for Madrid/Barajas station. At first glance, the effects of filtering

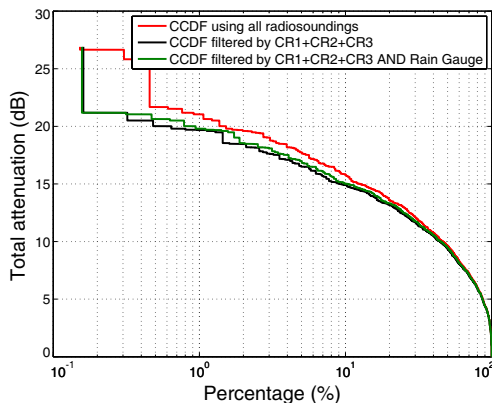


**Figure 5.** Set of three CCDFs of total attenuation at 300 GHz for Madrid/Barajas, year 2011.

out rain events detected with the proposed method seem to be less relevant in comparison to the behavior previously observed at 100 GHz. In comparison with results at that frequency, it can be certainly observed that, in relative terms, the variations with respect to the CCDFs computed from all radiosoundings are not so significant. The explanation to this observation can be found in the strong absorption effects of atmospheric gases at 300 GHz. Regarding to the comparison between the two filtered CCDFs, it can be immediately verified that both distributions have a high degree of similarity between each other, as in the analysis carried out at 100 GHz.

The effects of the rain events detected from the rain gauge data but missed with the proposed method were also analyzed at both frequencies. New CCDFs were calculated discarding also the rain events detected uniquely by the rain gauge. The resulting CCDFs are highly coincident with the CCDFs derived from radiosoundings filtered by the method. This confirms that rain events registered by the rain gauge but not detected by the proposed method are of little relevance for attenuation statistics under non-precipitation conditions.

## 5. 5-YEAR STATISTICS OF TOTAL ATTENUATION AT 100 AND 300 GHz

The results of using the proposed rain detection method on the processing of yearly statistics of attenuation are illustrated in this section. With this purpose, a 5-year analysis has been performed, based on RAOBs corresponding to the years between 2007 and 2011

in Madrid/Barajas.

CCDFs of total attenuation  $A_T$  for 5 years have been calculated and plotted both at 100 GHz (see Fig. 6(a)) and 300 GHz (see Fig. 6(b)). The statistics have been obtained by filtering out those RAOBs identified as carried out during rainy conditions. Besides, the CCDF computed with all RAOBs for 2007, at the two frequencies of interest, is also plotted in the corresponding graph. Both have been included with the aim of comparing the result of filtering out the detected rain events with examples of CCDFs for which these events have not been filtered. The unfiltered curves for the rest of the yearly periods are not plotted, since their behavior have been observed as quite similar. A summary of the number of RAOBs discarded in each period is given in Table 5.

The number of events identified are reasonably close, except for year 2010 where a higher presence of rainy conditions has been detected. However, this higher presence of rain in 2010 apparently does not have a remarkable effect on the yearly statistics, in comparison to the rest of the years, as it is observed in Figs. 6(a) and 6(b).

At 100 GHz, cumulative distributions as well as the total attenuation levels are moderately similar in the five years. Predicted values of  $A_T$  exceeded between 1 and 10% of time are in the order of 1.8 and 2.8 dB. It is also remarkable that, after discarding rain events, the total attenuation exceeded 20% of time is quite similar and about 1.3 dB for every period, which could be considered as a consistent validation of the good performance of our method for different sets of data at the same location. For percentages of time below 1%, tails

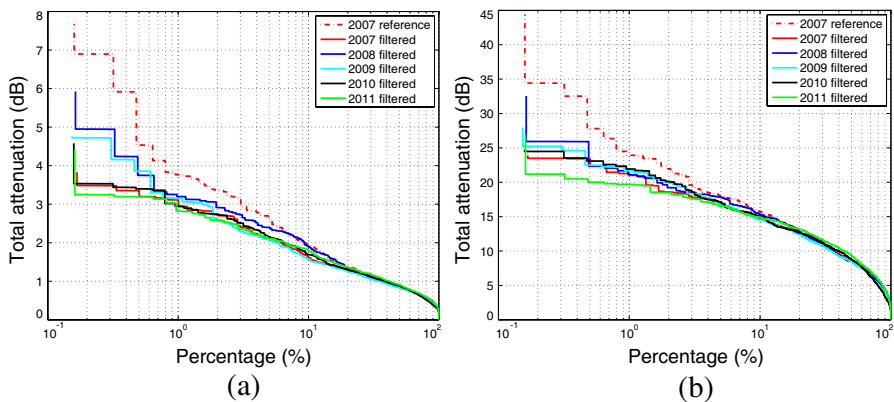


**Figure 6.** Set of 5 filtered CCDFs of total attenuation at (a) 100 GHz and (b) 300 GHz for Madrid/Barajas. Years 2007–2011.

**Table 5.** Summary of 5-year analysis in Madrid/Barajas station.

Period	Total RAOBs with SYNOP	Rainy events detected by the method
2007	628	31
2008	656	43
2009	694	42
2010	695	63
2011	659	38

with higher attenuation values are observed on the distributions. As it was mentioned in Section 4, isolated cloud events characterized by high ILWC values are responsible of this particularity. Some divergences are also observed at these low percentages because the number of events becomes very small below 1% of time.

The strong effect of gaseous attenuation at 300 GHz is again observed on the five filtered CCDFs of estimated total attenuation. According to the results shown in Fig. 6(b), below 10% of time it is expected that predicted values of  $A_T$  exceed about 15 dB of atmospheric losses, reaching even higher values, in the order of 20 to 23 dB for 1% of time. Variations observed with respect to the CCDFs calculated with all RAOBs are less significant at this frequency. The effect of high ILWC events seems not having relevant influence, due to the dominant impact of gaseous absorption at this frequency.

## 6. CONCLUSIONS

In the framework of an atmospheric propagation study at 100 and 300 GHz, under non-scattering conditions, based on the analysis of radiosonde observations (RAOBs), the need has arisen to identify and filter out those RAOBs carried out during precipitation conditions, for which the used absorption models are not adequate. Thus, a method is proposed in order to identify rainy conditions, which is based on a set of identification criteria defined, in turn, by an analysis of parameters extracted from concurrent SYNOP reports, coupled with an auxiliary ILWC threshold in order to refine the procedure. With the aim of evaluating the accuracy of the method, an exhaustive comparative study has been carried out using colocated rain gauge data, which was considered as the most reliable source of identification of rain events during the radiosonde launching. With this purpose, meteorological information was collected from weather stations in Spain placed in Madrid/Barajas, Murcia and Santander, characterized

by different climate conditions. In order to estimate attenuation values from vertical profiles collected from RAOBs, the line-by-line method included in ITU-R Rec. P.676 was combined with Salonen cloud detection model.

After the definition and evaluation of the method, it can be concluded that, in the absence of rain gauge data, the proposed identification method can be considered as an adequate and useful procedure to filter out those radiosounding events probably carried out under rainy conditions. In general, the method can be considered as a conservative detection tool because, as it has been verified, the number of events to be discarded is always higher than the observed by the colocated rain gauge. Thus, it could be concluded that the method overestimates the presence of rain during the year, nevertheless, this fact does not have a relevant impact when CCDFs of estimated total attenuation filtered by the proposed method or by the rain gauge data are compared.

Finally, it is expected that yearly cumulative statistics of total attenuation filtered by the proposed method, would be closest to the ones obtained from long-term experimental measurements campaigns under clear sky or cloudy conditions. Indeed, filtered CCDFs obtained give an interesting and valuable tool in order to understand the limits of the propagation at 100 and 300 GHz through the atmosphere.

In order to extend the validity of these conclusions and to observe the behavior of the method under different climates, additional tests could be carried out in other geographical regions out of Spain.

## ACKNOWLEDGMENT

This work is supported by the Ministry of Science and Innovation of Spain, under projects Consolider-Ingenio 2010 CSD2008-00068 (TeraSense) and TEC-2010-19241-C02-01.

## REFERENCES

1. Siegel, P. H., "Terahertz technology," *IEEE Transactions on Microwave Theory and Techniques*, Vol. 50, No. 3, 910–928, 2002.
2. Tonouchi, M., "Cutting-edge terahertz technology," *Nature Photonics*, Vol. 1, No. 2, 97–105, 2007.
3. Zhou H., F. Ding, Y. Jin, and S. He, "Terahertz metamaterial modulators based on absorption," *Progress In Electromagnetics Research*, Vol. 119, 449–460, 2011.

4. Xu, O., "Diagonal horn gaussian efficiency enhancement by dielectric loading for submillimeter wave application at 150 GHz," *Progress In Electromagnetics Research*, Vol. 114, 177–194, 2011.
5. Dou, W.-B., H. F. Meng, B. Nie, Z.-X. Wang, and F. Yang, "Scanning antenna at THz band based on quasi-optical techniques," *Progress In Electromagnetics Research*, Vol. 108, 343–359, 2010.
6. Kulesa, C., "Terahertz spectroscopy for astronomy: From comets to cosmology," *IEEE Transactions on Terahertz Science and Technology*, Vol. 1, No. 1, 232–240, 2011.
7. Yeom, S., D. Lee, H. Lee, J. Son, and V. P. Gushin, "Distance estimation of concealed objects with stereoscopic passive millimeter-wave imaging," *Progress In Electromagnetics Research*, Vol. 115, 399–407, 2011.
8. Kemp, M., "Explosives detection by terahertz spectroscopy — A bridge too far?" *IEEE Transactions on Terahertz Science and Technology*, Vol. 1, No. 1, 282–292, 2011.
9. Siegel, P. H., "Terahertz technology in biology and medicine," *IEEE Transactions on Microwave Theory and Techniques*, Vol. 52, No. 10, 2438–2447, 2004.
10. Ajito, K. and Y. Ueno, "THz chemical imaging for biological applications," *IEEE Transactions on Terahertz Science and Technology*, Vol. 1, No. 1, 293–300, 2011.
11. Cimini, D., R. Westwater, A. J. Gasiewski, M. Klein, V. Y. Leuski, and J. C. Liljegren, "Ground-based millimeter-and submillimeter-wave observations of low vapor and liquid water contents," *IEEE Transactions on Geoscience and Remote Sensing*, Vol. 45, No. 7, 2169–2180, 2007.
12. Luini, L., C. Riva, C. Capsoni, and A. Martellucci, "Attenuation in nonrainy conditions at millimeter wavelengths: Assessment of a procedure," *IEEE Transactions on Geoscience and Remote Sensing*, Vol. 45, No. 7, 2150–2157, 2007.
13. Das, S., A. Maitra, and A. K. Shukla, "Rain attenuation modeling in the 10–100 GHz frequency using drop size distributions for different climatic zones in tropical India," *Progress In Electromagnetics Research B*, Vol. 25, 211–224, 2010.
14. Owolawi, P. A., "Rainfall rate probability density evaluation and mapping for the estimation of rain attenuation in south africa and surrounding islands," *Progress In Electromagnetics Research*, Vol. 112, 155–181, 2011.
15. Terasense, "TeraSense: Project summary," 2012, <http://www.ter>

- asense.org.
16. Liebe, H., G. Hufford, and M. Cotton, "Propagation modeling of moist air and suspended water/ice particles at frequencies below 1000 GHz," *AGARD, 52nd Specialists Meeting of the Electromagnetic Wave Propagation Panel*, Vol. 1, 1993.
  17. Rosenkranz, P., "Water vapor microwave continuum absorption: A comparison of measurements and models," *Radio Science*, Vol. 33, No. 4, 919–928, 1998.
  18. Siles, G., J. Riera, and P. García-del-Pino, "Considerations on cloud attenuation at 100 and 300 GHz for propagation measurements within the TeraSense project," *Proceedings of the 5th European Conference on Antennas and Propagation (EUCAP)*, 2011.
  19. Salonen, E. and S. Uppala, "New prediction method of cloud attenuation," *Electronics Letters*, Vol. 27, No. 12, 1106–1108, 1991.
  20. Decker, M., E. Westwater, and F. Guiraud, "Experimental evaluation of ground-based microwave radiometric sensing of atmospheric temperature and water vapor profiles," *Journal of Applied Meteorology*, Vol. 17, No. 12, 1788–1795, 1978.
  21. Mattioli, V., P. Basili, S. Bonafoni, P. Ciotti, and E. Westwater, "Analysis and improvements of cloud models for propagation studies," *Radio Science*, Vol. 44, No. 2, 2009.
  22. University of Wyoming, "Upper air data: Soundings," 2012, <http://weather.uwyo.edu/upperair/sounding.html>.
  23. Durre, I., R. Vose, and D. Wuertz, "Overview of the integrated global radiosonde archive," *Journal of Climate*, Vol. 19, No. 1, 53–68, 2006.
  24. Bosisio, A., E. Fionda, P. Basili, G. Carlesimo, and A. Martellucci, "Identification of rainy periods from ground based microwave radiometry," *European Journal of Remote Sensing*, Vol. 45, 41–50, 2012.
  25. World Meteorological Organization, *Manual on Codes — International Codes, Part A*, 2010.
  26. Turner, D., A. Vogelmann, R. Austin, J. Barnard, K. Cady-Pereira, J. Chiu, S. Clough, C. Flynn, M. Khaiyer, J. Liljegren, et al., "Thin liquid water clouds," *Bulletin of the American Meteorological Society*, Vol. 88, No. 2, 177–190, 2007.
  27. Al-Ansari, K., P. García-del-Pino, J. Riera, and A. Benarroch, "One-year cloud attenuation results at 50 GHz," *Electronics Letters*, Vol. 39, No. 1, 136–137, 2003.

28. Siles, G., J. Riera, and P. García-del-Pino, "Estimation of total attenuation at 100 and 300 GHz using meteorological data in madrid," *Proceedings of the ESA/ESTEC Workshop on Radiowave Propagation*, 2011.
29. Radiosonde EU, "Stations de radiosondage en Espagne," (Radiosounding stations in Spain), 2012, <http://www.radiosonde.eu/RS02/RS02K.html>.
30. García-del-Pino, P., R. Rial, M. Cruz Moro, and A. Benarroch, "Experimental  $0^\circ$  isotherm height in Spain: Comparison with predictions and application for rain attenuation," *Open Symposium on Propagation and Remote Sensing, URSI Commission-F*, 2002.
31. ITU-R, "ITU-R recommendation P.676-8. attenuation by atmospheric gases," 2009.
32. ITU-R, "ITU-R recommendation P.840-5. attenuation due to clouds and fog," 2012.
33. Siles, G., J. Riera, and P. García-del-Pino, "On the use of radiometric measurements to estimate atmospheric attenuation at 100 and 300 GHz," *Journal of Infrared, Millimeter and Terahertz Waves*, Vol. 32, 528–540, 2011.